Effect of Salt on Self-Assembly in Charged Block Copolymer Micelles

O. V. Borisov*,†,‡ and E. B. Zhulina†,§

Institute of Macromolecular Compounds of the Russian Academy of Sciences, 199004, St. Petersburg, Russia; LRMP/UMR 5067, Helioparc Pau-Pyrenees, 64053 Pau, France; and Department of Chemistry and Biochemistry and Center for Polymer Research, The University of Texas at Austin, Austin, Texas 78712

Received May 30, 2001; Revised Manuscript Received January 30, 2002

ABSTRACT: We consider self-assembly of block copolymers with one charged (polyelectrolyte) and one hydrophobic block in a salt-added solution. In the case of short hydrophobic and long polyelectrolyte block the copolymers form starlike polyelectrolyte micelles, while in the opposite case so-called crew-cut micelles are found. Upon an increase in the salt concentration the number of chains in a micelle increases, while the radius of the micellar corona weakly decreases due to enhanced screening of the Coulomb repulsion between the charged blocks. The exponents of the corresponding power-law dependences are obtained on the basis of scaling arguments and compared to the experimental observation.

1. Introduction

Block copolymers with one polyelectrolyte and one hydrophobic block (or hydrophobically end-modified polyelectrolytes) can be viewed as ionic polymeric surfactants. The adsorption of hydrophobic blocks on a solid substrate as well as their anchoring at water−air and water−oil interfaces gives rise to monolayers or polyelectrolyte brushes formed by water-soluble blocks. Such structures have been extensively studied both theoretically[1−4] and experimentally[5−8] during the past decade due to their diverse industrial and biomedical applications.[9,10]

Alternatively, the hydrophobically modified polyelectrolytes can associate in micelle-like aggregates of different morphologies. The self-assembly of charged block copolymers in the solution at concentrations above the critical association concentration (CAC) results in the formation of aggregates consisting of a dense hydrophobic core formed by insoluble blocks and the extended charged corona, which ensures solubility of micelles in water.[11] We refer to these aggregates as "polyelectrolyte micelles". Depending on the geometry, the coronae of such micelles can be envisioned as curved polyelectrolyte brushes[1,2,4] or regularly branched[12,13] (star- or comblike) polyelectrolytes.

The association equilibrium and the structure of micelles formed by block copolymers with charged soluble block are governed by the competition between hydrophobic attraction of insoluble blocks and the Coulomb repulsion between charged monomers in the micellar coronae. The latter interaction is strongly mediated by the counterions which are always present in the solution to ensure its electroneutrality as a whole.

The equilibrium structure of the polyelectrolyte micelles formed in a salt-free solution has been analyzed in refs 14−17. However, the screening effects which arise in a salt-added solution and even in a salt-free solution close to CAC remained mostly out of the scope of these earlier studies or were underestimated[18] (see discussion in ref 13 for details).

The goal of this paper is to analyze systematically how the ionic strength of the solution (controlled by the concentration of added low-molecular-weight salt) affects the CAC and the equilibrium characteristics of spherical micelles. Our analysis employs the scaling model which was developed in our earlier studies of the charged polymer stars[13] and polyelectrolyte brushes.[2,3] In the framework of this model we calculate the free energy of a spherical polyelectrolyte micelle and obtain its equilibrium characteristics as a function of the ionic strength in the solution. We focus on the main experimentally measurable properties of the micelles: the aggregation number p (the number of chains associated into one micelle) and the micelle overall size.

The rest of the paper is organized as follows. In section 2, we describe the model of a charged spherical micelle. In section 3, we review the results for neutral starlike and crew-cut micelles. In section 4, the structure of the charged starlike micelles in the salt-free and salt-added solutions is considered, and the equilibrium parameters of micelles and CAC are obtained. In section 5, we analyze the crew-cut polyelectrolyte micelles, and in section 6, we summarize our results and conclusions.

2. Model

We consider a dilute solution of block copolymers, each comprising a hydrophobic block with the degree of polymerization N_B and a polyelectrolyte block with the degree of polymerization N_A. Both blocks are assumed to be intrinsically flexible (the statistical segment length is of the order of a monomer unit length a, which is taken as the unit length in our subsequent analysis), and the polyelectrolyte block is weakly charged, i.e., comprises the fraction $\alpha \ll (a/l_B)^2 \cong 1$ of charged monomers. Here $l_B = e^2/k_BT\epsilon$ is the Bjerrum length, which is of order 0.7 nm in water under normal conditions (e is the elementary charge, ϵ is the dielectric constant of the solvent, T is the temperature, and k_B is the Boltzmann constant). The fraction α of charged monomers in the A-block is assumed to be quenched, i.e., independent of the external conditions. Because of the electroneutrality condition, the solution contains also counterions which, in total, compensate the overall charge of ionic blocks of copolymers and, in the general case, also salt. The salt concentration, c_s, in the bulk of

† Institute of Macromolecular Compounds of the Russian Academy of Sciences.
‡ LRMP/UMR 5067.
§ The University of Texas at Austin.

10.1021/ma010934n CCC: $22.00
Published on Web 04/19/2002

the solution determines the Debye screening length, $r_D \cong (l_B c_s)^{-1/2}$.

The nonelectrostatic, short-range interactions between uncharged monomer units are described by the dimensionless second, v_A, v_B, and the third, w_A, w_B, virial coefficients which are normalized by the factors a^{-3} and a^{-6}, respectively. As water is a poor solvent for the hydrophobic B-block, v_B is negative and proportional to the relative deviation form the θ-temperature, $v_B \cong -\tau_B \equiv (\theta_B - T)/\theta_B \leq 0$. (We remark that usually the solubility of hydrophobic polymers in water decreases upon an increase in T.) On the contrary, for uncharged monomer units of a polyelectrolyte block water is assumed to be a marginal good or Θ-solvent, i.e., $v_A \cong 0$. This approximation is justified because the dominant contribution to the interactions in the micellar coronas is provided by the Coulomb repulsion. The third virial coefficient, w, which is virtually independent of T, is of order of unity.

At concentrations above CAC the block polyelectrolyte chains associate to form micelles. In these micelles the hydrophobic blocks stick together to form the dense core (the density of the core is $\sim\tau_B$) while the polyelectrolyte blocks remain in water phase and form the micellar corona. In our analysis we consider the charged corona of the micelle as a polyelectrolyte star (if the core radius is much smaller than the overall size of the corona) or as a curved polyelectrolyte brush in the opposite case. This enables us to use the earlier results obtained in refs 2−4,12, and 13 to calculate the free energy of a micellar corona.

The free energy of a chain in a micelle with aggregation number p yields

$$F(p) = F_{corona}(p) + F_{core}(p) + F_{surface}(p) \qquad (1)$$

and comprises the coronal contribution, $F_{corona}(p)$, the entropic penalty for the extension of the hydrophobic blocks in the micellar core, $F_{core}(p)$, and the excess free energy of the micellar core/water interface, $F_{surface}(p)$.

Minimization of the free energy, eq 1, with respect to the aggregation number p enables us to find the number p_{eq} of associated block copolymers and the free energy of a chain in the equilibrium micelle. The CAC can be found from the condition of equality of chemical potentials of a chain in associated and dissociated states, i.e., $\mu^{(diss)}(c) = \mu^{(ass)}(c)$ at c = CAC, which results in

$$\ln \text{CAC} \approx (F(p_{eq}) - F(p{=}1))/k_B T \qquad (2)$$

We note that this approach is an extension of an earlier one[19,20] based on the scaling model[21−24] of neutral block copolymer micelles.

3. Neutral Block Copolymer Micelles

As an important reference point for our subsequent analysis, we review first the main results of the scaling theory of micelles formed by block copolymers with neutral soluble blocks.[19,20] In the case of strongly asymmetric block copolymers ($N_A \gg N_B$) the size of the micellar core, $R_{core}(p) \cong (pN_B/\tau_B)^{1/3}$, is much smaller than the radius, R_{corona}, of the micellar corona, so that the micelle is reminiscent of the starlike polymer (see Figure 1a). In the framework of the scaling theory, the corona of the starlike micelle can be envisioned[21,22] as an array of concentric spherical shells of close-packed blobs. The condition of close packing imposes the blob size, $\xi(r) \cong rp^{-1/2}$, equal to the average distance between the coronal blocks (here r is the distance from the center of the micelle). Each blob corresponds to the $\sim k_B T$ contribution to the free energy of steric repulsion between the coronal chains. After calculating the total number of blobs in the micellar corona, one finds the free energy of steric repulsion (per chain) as

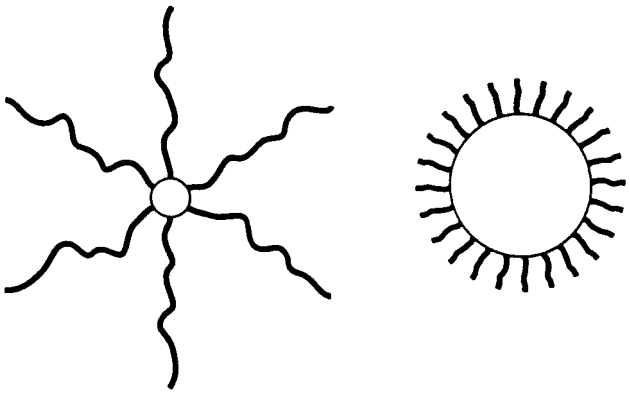

Figure 1. Starlike (a) and crew-cut (b) block copolymer micelle. $p \geq 1$ is the aggregation number, N_A is the number of monomers in the hydrophilic block, and N_B is the number of monomers in the hydrophobic block.

$$F_{corona}(p)/k_B T \cong p^{1/2} \ln \frac{R_{corona}}{R_{core}} \qquad (3)$$

where $R_{corona} \cong N_A^{3/5} v_A^{1/5} p^{1/5}$ and $R_{corona} \cong N_A^{1/2} p^{1/4}$ under good or θ-solvent conditions for coronal chains, respectively. The excess free energy of the core−water interface is given by

$$F_{surface}(p)/k_B T \cong \gamma s \cong (N_B \tau_B^{\,2})^{2/3} p^{-1/3} \qquad (4)$$

where $k_B T\gamma \cong k_B T \tau_B^2$ is the surface tension at the core−water interface and

$$s \cong R_{core}^{\,2}(p)/p \cong (N_B/\tau_B)^{2/3} p^{-1/3} \qquad (5)$$

is the area of the core−water interface per chain. For strongly asymmetric copolymers the third contribution, F_{core}, is negligible, and the minimization of $F_{corona}(p) + F_{surface}(p)$ with respect to p results in an equilibrium aggregation number

$$p_{eq} \cong (N_B \tau_B^{\,2})^{4/5} \left(\ln \frac{R_{corona}}{R_{core}} \right)^{-6/5} \qquad (6)$$

An important feature of eq 6 is an absence of the power-law dependence of the aggregation number p_{eq} on the length N_A of the coronal block.

In the opposite limit of short polyelectrolyte blocks, $N_A \ll N_B$, the size of the micellar core, $R_{core}(p)$, exceeds by far the thickness of the corona. The coronae of these so-called crew-cut micelles can be viewed as quasi-planar polymer brushes[23,24] (Figure 1b). The thickness of the corona $H_{corona} = R_{corona} - R_{core}$ scales as $H_{corona} \cong N_A v_A^{1/3} s^{-1/3}$ or $H_{corona} \cong N_A s^{-1/2}$ while the number of the coronal blobs per chain $\sim H_{corona}/\xi$ is proportional to the free energy of the interchain repulsion and equals $F_{corona}/k_B T \cong N_A v_A^{1/3} s^{-5/6}$ or $F_{corona}/k_B T \cong N_A s^{-1}$ under good and Θ-solvent conditions for the coronal chains, respectively. Taking into account eq 5 and minimizing the free energy with respect to p, we obtain the equi-

librium aggregation number for the crew-cut micelles: $p_{eq} \cong N_B^2 \tau_B^{14/11} N_A^{-18/11} v_A^{-6/11}$ (good solvent) and $p_{eq} \cong N_B^2 \tau_B N_A^{-3/2}$ (Θ solvent). In contrast to the case of starlike micelles, the equilibrium aggregation number in the crew-cut micelles strongly decreases upon an increase in the degree of polymerization of the soluble blocks because of their stronger interaction.

4. Starlike Polyelectrolyte Micelles

The starlike polyelectrolyte micelles are formed by strongly asymmetric copolymers with short hydrophobic and long polyelectrolyte block. Below we calculate the interaction free energy in the polyelectrolyte micellar corona on the basis of a scaling model developed in refs 12 and 13.

4.1. Salt-Free Solution. 4.1.1. Structure of the Micellar Corona. We start our analysis from the case, when the solution contains only copolymers and counterions but no salt. The equilibrium distribution of mobile counterions inside and outside the corona and the extension of the coronal chains are determined by the balance of (i) Coulomb interactions between all the charges (charged monomers and counterions), (ii) translational entropy of counterions, and (iii) conformational entropy penalty for the extension of the coronal chains.

The counterions spread fairly uniformly over the whole volume of the solution, if the number of coronal chains (the aggregation number in our case) is small, i.e., $p \le \alpha^{-1/2} l_B^{-1}$. The balance of the energy of the unscreened Coulomb repulsion, $F_{Coulomb}/k_BT \cong l_B(p\alpha N_A)^2/R_{corona}$, and the conformational entropy penalty for the extension of the coronal chains, $F_{conf}/k_BT \cong pR_{corona}^2/N_A$, results in the extension of the coronal chains up to $R_{corona} \cong N_A(\alpha^2 l_B)^{1/3} p^{1/3}$.

On the contrary, when the number of chains associated into a micelle is large, $p \ge \alpha^{-1/2} l_B^{-1}$, the energy of the Coulomb attraction of counterions to the charged corona is strong enough to retain most of the counterions inside the coronal space. This effect known as "charge renormalization" has been first proposed for charged colloidal particles by Alexander et al.[25] The Coulomb repulsion between the coronal chains is strongly screened and their extension, $R_{corona} \cong N_A\alpha^{1/2}$, is determined primarily by the osmotic pressure of trapped inside the corona counterions.

Each polyelectrolyte chain in the micellar corona can be envisioned as a string of electrostatic blobs of equal size,

$$\xi(p) \cong \begin{cases} (\alpha^2 l_B)^{-1/3} p^{-1/3}, & p \ll \alpha^{-1/2} l_B^{-1} \\ \alpha^{-1/2} & p \gg \alpha^{-1/2} l_B^{-1} \end{cases} \qquad (7)$$

which are not close packed (Figure 2a). Because of the interchain Coulomb repulsion, the blob size in the micellar corona is smaller than that in an individual polyelectrolyte chain: $\xi(p) \le \xi(p=1) \equiv \xi_e \cong (\alpha^2 l_B)^{-1/3}$. The presentation of the coronal chains as strings of electrostatic blobs of constant size (eq 7) applies except for the region proximal to the core, $r \le p^{1/2}\xi(p) \equiv \rho(p)$. Here, the polymer concentration is sufficiently high to ensure predominance of the nonelectrostatic (steric) interactions over the electrostatic ones, and the blobs are close packed just as in the corona of a neutral micelle. Clearly, the proximal region exists, if the core is sufficiently small, $R_{core} \le \rho(p)$.

4.1.2. Micellization in a Salt-Free Solution. The coronal contribution to the free energy for a micelle with a small aggregation number, $p \le \alpha^{-1/2} l_B^{-1}$, is equal to the energy of Coulomb repulsion between the coronal chains and can be simply estimated as the number of coronal electrostatic blobs per chain,

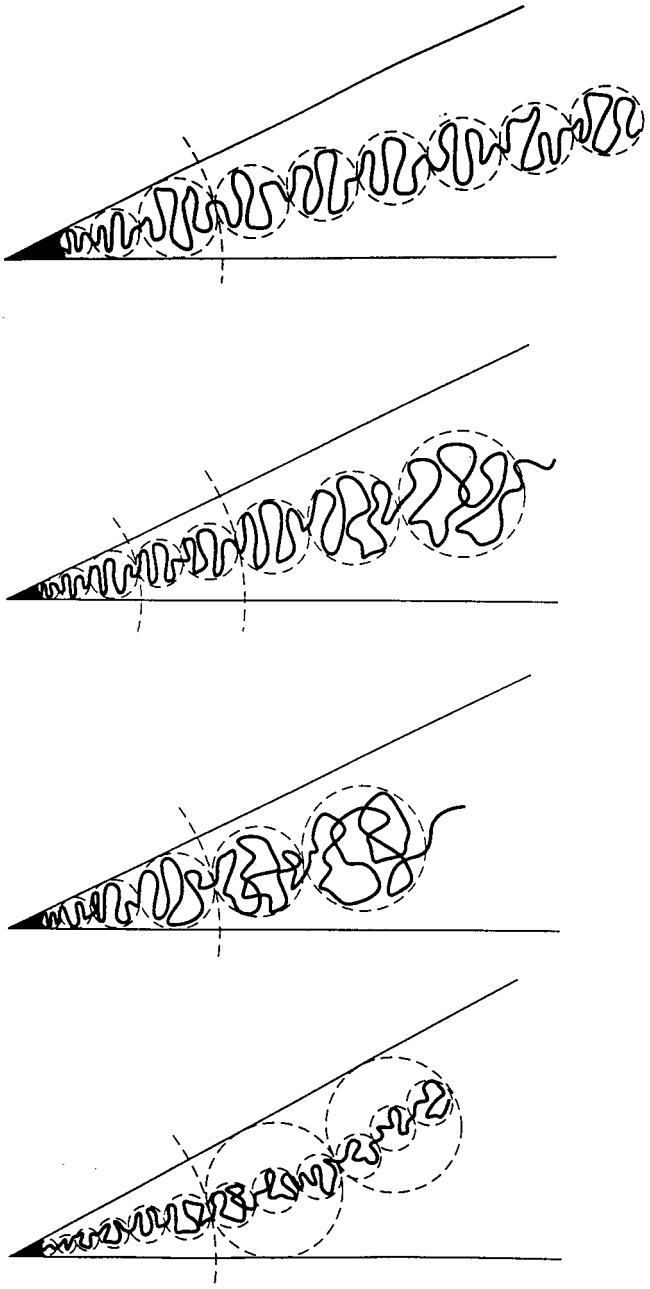

Figure 2. Blob picture of the starlike micellar corona at $c_s \le c_s^{(1)}$ (a), $c_s^{(1)} \le c_s \le c_s^{(2)}$ (b), $c_s^{(2)} \le c_s \le \alpha^{3/2}$ (c), and $\alpha^{3/2} \le c_s \le c_s^{(3)}$ (d).

$$\frac{F_{corona}(p)}{k_BT} \cong \frac{R_{corona}(p)}{\xi(p)} \cong N_A(\alpha^2 l_B)^{2/3} p^{2/3}, \quad p \ll \alpha^{-1/2} l_B^{-1} \qquad (8)$$

The free energy of the corona at $p \ge \alpha^{-1/2} l_B^{-1}$ comprises also the translational entropy penalty for the localization of αN counterions per chain within the corona. As a result, we get

$$F_{corona}(p)/k_BT \cong N_A\alpha \ln(pN_A\alpha/R_{corona}^3), \quad p \gg \alpha^{-1/2} l_B^{-1} \qquad (9)$$

The minimization of the overall free energy per chain in a micelle, $F_{coronal} + F_{interface}$, given by eqs 8, 9, and 4 leads to the following expressions for the aggregation number

$$p_{eq} \cong \begin{cases} (N_B\tau_B{}^2)^{2/3} N_A{}^{-1} (\alpha^2 l_B)^{-2/3}, & \mathcal{K} \ll 1 \\ (N_B\tau_B{}^2)^2 (N_A\alpha)^{-3}, & \mathcal{K} \gg 1 \end{cases} \quad (10)$$

and for the size of corona

$$R_{corona,\,eq} \cong \begin{cases} N_A{}^{2/3} (\alpha^2 l_B)^{1/9} (N_B\tau_B{}^2)^{2/9}, & \mathcal{K} \ll 1 \\ N_A \alpha^{1/2}, & \mathcal{K} \gg 1 \end{cases} \quad (11)$$

where we have introduced the characteristic ratio $\mathcal{K} \equiv N_B{}^2\tau_B{}^4 l_B / N_A{}^3 \alpha^{5/2}$. Hence, depending on the value of $\mathcal{K}$, either "small" unscreened micelles (at $\mathcal{K} \ll 1$) or large, osmotic micelles (at $\mathcal{K} \gg 1$) are formed above CAC. As one can expect, the aggregation number appears to be a strongly decreasing function of the degree of polymerization and the fraction of charged monomers in the coronal A-block. As a result, starlike polyelectrolyte micelles are expected to be marginally stable in salt-free solutions.

The chemical potential of a chain in the dissociated state reads

$$\mu^{(diss)}(c) \cong \ln c + \alpha N_A \ln(\alpha N_A c) + N_A (\alpha^2 l_B)^{2/3} + (N_B\tau_B{}^2)^{2/3} \quad (12)$$

where c is the concentration of polymer chains in the solution; the first and the second terms account for translational entropy of the chain and of the counterions, respectively; the third term describes the free energy of the extension of the A-block, and the last term is the excess interfacial energy of the collapsed B-block. The chemical potential of a chain in the associated state yields

$$\mu^{(ass)}(c) \cong \begin{cases} \alpha N_A \ln(\alpha N_A c) + N_A (\alpha^2 l_B)^{2/3} p_{eq}{}^{2/3} + (N_B\tau_B{}^2)^{2/3} p_{eq}{}^{-1/3}, & \mathcal{K} \ll 1 \\ \alpha N_A + \alpha N_A \ln(\alpha N_A p_{eq} / R_{corona,eq}{}^3) + (N_B\tau_B{}^2)^{2/3} p_{eq}{}^{-1/3}, & \mathcal{K} \gg 1 \end{cases} \quad (13)$$

where the equilibrium aggregation number p_{eq} and the radius of the corona $R_{corona,\,eq}$ are given by eqs 10 and 11, respectively. Using eqs 12 and 13 and keeping only the leading terms, we find

$$\ln(\mathrm{CAC}) \cong \begin{cases} (N_B\tau_B{}^2)^{2/3} + N_A{}^{1/3} (\alpha^2 l_B)^{2/9} (N_B\tau_B{}^2)^{4/9}, & \mathcal{K} \ll 1 \\ -(N_B\tau_B{}^2)^{2/3} (\alpha N_A)^{-1} + \ln[(N_B\tau_B{}^2)^2 N_A{}^{-6} \alpha^{-9/2}], & \mathcal{K} \gg 1 \end{cases} \quad (14)$$

The appearance of the factor $(\alpha N_A)^{-1}$ in the first (negative) term in the case of osmotic micelles, $\mathcal{K} \gg 1$, is related to the entropic penalty for the localization of counterions upon micellization.[26] This effect results in significant increase in the CAC as has been discussed earlier in context of condensation of counterions on the surfactant micelles.[27]

4.2. Salt-Added Solution. 4.2.1. Structure and Free Energy of the Corona. The screening effect of salt in the corona of a micelle with a small aggregation number, $p \le \alpha^{-1/2} l_B{}^{-1}$, becomes important when $r_D \le R_{corona}$, i.e., when

$$c_s \ge c_s^{(1')} \equiv p^{-2/3} \alpha^{-4/3} l_B{}^{-5/3} N_A{}^{-2}, \quad p \le \alpha^{-1/2} l_B{}^{-1}$$

For the osmotic micelles comprising large number of chains, $p \ge \alpha^{-1/2} l_B{}^{-1}$, the onset of the screening effect of salt occurs at

$$c_s \ge c_s^{(1)} \equiv p\alpha^{-1/2} N_A{}^{-2}, \quad p \ge \alpha^{-1/2} l_B{}^{-1}$$

which corresponds to the equality of the bulk salt concentration, c_s, and the average concentration of counterions in the micellar corona.

At higher salt concentration the corona can be subdivided into several concentric regions which differ with respect to radial dependences for the local structural properties. In Figure 3 the positions of the boundaries between the regions are plotted as a function of salt concentration c_s. Two additional characteristic salt concentrations

$$c_s^{(2)} \equiv p l_B{}^{-5/3} \alpha^{-4/3} N_A{}^{-2}$$

$$c_s^{(3)} \equiv \alpha^{4/3} l_B{}^{-1/3}$$

can be introduced; as follows from the subsequent discussion, they correspond to crossovers between different structural regimes for the micellar corona.

We analyze first the salt-induced evolution of the coronae of the osmotic micelles, $p \ge \alpha^{-1/2} l_B{}^{-1}$; in the end of the section we briefly discuss the case of micelles with small, $p \le \alpha^{-1/2} l_B{}^{-1}$ aggregation numbers.

Salt Range $c_s^{(1)} \le c_s \le c_s^{(2)}$. The micellar corona comprises (i) the proximal region, $R_{core} \le r \le \rho(p)$, dominated by nonelectrostatic interactions, (ii) the region of uniform extension, $\rho(p) \le r \le r_s$, where the local concentration of counterions $c_i(r)$ is still higher than the salt concentration in the bulk of the solution, c_s, and (iii) the peripheral, affected by salt, region $r_s \le r \le R_{corona}(c_s)$ (Figure 2b). The position of the boundary, r_s, between the affected by salt periphery of the corona and the region of the uniform extension is given by $r_s \cong (p\alpha^{1/2})^{1/2} c_s{}^{-1/2}$; it is displaced toward the center of the micelle upon an increase in c_s.

In the affected by salt extremity of the corona the chain extension decreases in the radial direction. This

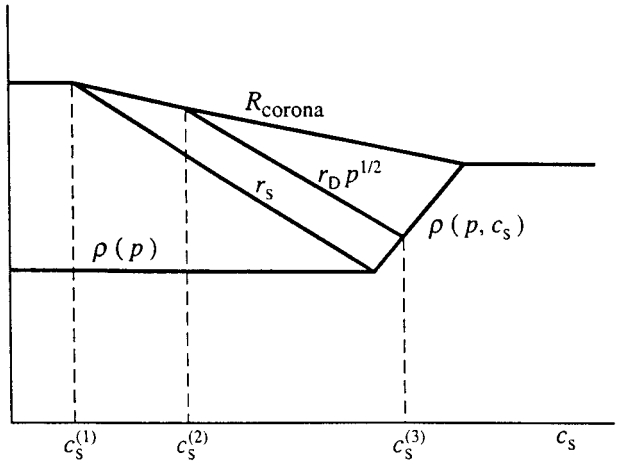

Figure 3. Evolution of the boundaries of different regions of the micellar corona as a function of salt concentration.

is reflected in a sublinear growth of the blob size as a function of r,

$$\xi(r) \cong (\alpha^2 p)^{-1/3} c_s^{1/3} r^{2/3} \tag{15}$$

as illustrated in Figure 2b.

The radius of the corona $R_{corona}(c_s)$ is determined by the condition of conservation of the total number of monomers as

$$pN_A \cong \int_{R_{core}}^{R_{corona}} c_A(r) r^2 \, dr \tag{16}$$

where

$$c_A(r) \cong \begin{cases} p^{1/2}/r, & R_{core} \le r \le \rho(p) \\ p\xi(r)/r^2, & \rho(p) \le r \le R_{corona} \end{cases} \tag{17}$$

is the polymer density profile in the micellar corona and the blob size $\xi(r)$ is given by eq 7 at $\rho(p) \le r \le r_s$ or by eq 15 at $r_s \le r \le R_{corona}(c_s)$, respectively.

The free energy of the corona (in the units of k_BT) can be evaluated as the total number of elastic blobs,

$$\frac{F_{corona}(p)}{k_BT} \cong p^{1/2} \ln \frac{\rho(p)}{R_{core}} + \int_{\rho(p)}^{R_{corona}(c_s)} \frac{dr}{\xi(r)} \tag{18}$$

At concentrations of salt $c_s \gg c_s^{(1)}$ the integral on the rhs in eq 16 is dominated by the upper limit. As a result, the radius of corona scales as

$$R_{corona}(c_s) \cong N_A^{3/5} (\alpha^2 c_s^{-1})^{1/5} p^{1/5} \tag{19}$$

while the rhs of eq 18 is dominated by the upper limit of the last integral to give

$$F_{corona}(p)/k_BT \cong (N_A p^2 \alpha^4 c_s^{-2})^{1/5} \tag{20}$$

With increasing salt concentration, c_s, the dimensions of the coronal blobs increase according to eq 15. At salt concentration $c_s \cong c_s^{(2)}$ the size of the outermost (the largest) coronal blob reaches the value of ξ_e. Simultaneously, the Debye screening length, $r_D \cong (l_B c_s)^{-1/2}$, becomes equal to the average distance $R_{corona}p^{-1/2}$ between the chains at the edge of the corona.

Salt Range $c_s^{(2)} \le c_s \le \alpha^{3/2}$. The region of growing blobs, whose size is given by eq 15, extends in the range $r_s \le r \le r_D p^{1/2}$. The interchain interactions in the peripheral part of the corona, $r_D p^{1/2} \le r \le R_{corona}$, is equivalent to the short-range repulsion with the renormalized excluded-volume parameter $v_A^{(eff)} \cong \alpha^2 c_s^{-1}$; each chain can be presented as a semiflexible chain of electrostatic blobs of size ξ_e with the effective segment length of order r_D (Figure 2c).

The radius of the corona follows from the conservation condition for the polymer density profile, eq 16, with

$$c_A(r) \cong \begin{cases} p^{1/2}/r, & R_{core} \le r \le \rho(p) \\ p\xi(r)/r^2, & \rho(p) \le r \le r_D p^{1/2} \\ p^{2/3} c_s^{1/3} \alpha^{-2/3}/r^{4/3}, & r_D p^{1/2} \le r \le R_{corona} \end{cases} \tag{21}$$

The integral in eq 16 is still dominated by the upper limit thus leading (in the main term) to eq 19 for the corona size. The free energy of the corona can be presented as

$$\frac{F_{corona}(p)}{k_BT} \cong p^{1/2} \ln \frac{\rho(p)}{R_{core}} + \int_{\rho(p)}^{r_D p^{1/2}} \frac{dr}{\xi(r)} + p^{1/2} \ln \frac{R_{corona}}{r_D p^{1/2}} \tag{22}$$

The rhs of eq 22 is dominated by the upper limit of the second integral to give

$$F_{corona}(p)/k_BT \cong p^{1/2} (\alpha^{4/3} l_B^{-1/3} c_s^{-1})^{1/2} \tag{23}$$

With increasing salt concentration both the lower, r_s, and the upper, $r_D p^{1/2}$, boundaries of the region of growing blobs decrease proportionally to $c_s^{-1/2}$ as long, as r_s remains larger than the radius $\rho(p)$ of the proximal region. The region of uniform extension shrinks and eventually disappears; that is, the crossover $r_s \cong \rho(p)$ occurs at salt concentration $c_s \cong \alpha^{3/2}$.

Salt Range $\alpha^{3/2} \le c_s \le c_s^{(3)}$. The proximal region merges with the region of growing blobs (Figure 2d). The boundary between these regions is given by $\rho(p,c_s) \cong p^{1/2}\alpha^{-2}c_s$. The monomer density in the corona obeys eq 21, where the blob size $\xi(r)$ is given by eq 15 in the range $\rho(p, c_s) \le r \le r_D p^{1/2}$.

Equation for the free energy of the corona assumes the form

$$\frac{F_{corona}(p)}{k_BT} \cong p^{1/2} \ln \frac{\rho(p,c_s)}{R_{core}} + \int_{\rho(p,c_s)}^{r_D p^{1/2}} \frac{dr}{\xi(r)} + p^{1/2} \ln \frac{R_{corona}}{r_D p^{1/2}} \tag{24}$$

The size of the corona scales according to eq 19, whereas the leading terms in $F_{corona}(p)$ scale according to eq 23.

Upon an increase in the salt concentration, the radius $\rho(p,c_s) \cong p^{1/2}\alpha^{-2}c_s$ of the proximal quasi-neutral region of close-packed blobs increases because of weakening of the Coulomb interactions in comparison to the steric repulsion (which remains unaffected by salt). As a result, the region $\rho(p,c_s) \le r \le r_D p^{1/2}$ of growing electrostatic blobs shrinks, and eventually its upper boundary $r_D p^{1/2}$ merges with the lower boundary $\rho(p,c_s)$, i.e., the region of sublinearly growing electrostatic blobs disappears at $c_s \cong c_s^{(3)}$.

Salt Range $c_s \ge c_s^{(3)}$. Finally, at salt concentration higher than $c_s^{(3)}$ the Debye length r_D becomes smaller than the electrostatic blob size ξ_e. This means that the electrostatic blobs do not exist anymore, and the screened Coulomb interaction between the charged monomers is now equivalent to the short-range excluded-volume repulsion with renormalized (effective) second virial coefficient $v_A^{(eff)} \cong \alpha^2 c_s^{-1}$. Therefore, the structure of a neutral micelle in a good solvent is recovered. The main contribution to the coronal free energy scales as

$$F_{corona}(p)/k_BT \cong p^{1/2} \ln \frac{R_{corona}(c_s)}{R_{core}} \tag{25}$$

where $R_{corona}(c_s)$ is given by eq 19 (cf. eq 3).

The described above picture of the evolution of the structure of the micellar corona upon an increase in salt concentration requires minor modification for the case of small, $p \le \alpha^{-1/2} l_B^{-1}$, micelles. At salt concentrations

$c_s^{(1')} \le c_s \le c_s^{(2)}$ the chains in the corona remain uniformly stretched, in the range $\rho(p) \le r \le r_D$, i.e., $r_s \equiv r_D$. The crossover $r_D \cong \rho(p)$ occurs at $c_s \cong \alpha^{4/3} l_B^{-1/3} p^{-1/3}$. At higher salt concentration the structure of the corona is equivalent to that described above for the case $c_s \ge \alpha^{3/2}$.

4.2.2. Parameters of Equilibrium Micelle and CAC. By making use of eqs 4, 20, 23, and 25, we can now calculate an equilibrium aggregation number p_{eq} as a function of salt concentration, c_s. Minimization of $F_{corona} + F_{interface}$ with respect to p gives

$$p_{eq}(c_s) \cong \begin{cases} (N_B\tau_B^2)^2(\alpha N_A)^{-3} & c_s \ll c_s^{(1)} \\ (N_B\tau_B^2)^{10/11}(\alpha^4 N_A)^{-3/11} c_s^{6/11}, & c_s^{(1)} \ll c_s \ll c_s^{(2)} \\ (N_B\tau_B^2)^{4/5}\alpha^{-4/5} l_B^{1/5} c_s^{3/5} & c_s^{(2)} \ll c_s \ll c_s^{(3)} \\ (N_B\tau_B^2)^{4/5}\ln(R_{corona}/R_{core})^{-6/5}, & c_s \gg c_s^{(3)} \end{cases} \quad (26)$$

provided that $p_{eq}(c_s=0) \ge \alpha^{-1/2} l_B^{-1}$ or $\mathcal{K} \ge 1$. When $\mathcal{K} \le 1$ or $p_{eq}(c_s=0) \le \alpha^{-1/2} l_B^{-1}$, the effect of salt is negligible as long as $c_s \le c_s^{(1')}$ and the equilibrium aggregation number obeys eq 10.

As follows from eq 26, the number of chains in the equilibrium micelle increases as a power-law function of the salt concentration in the range $c_s^{(1)} \ll c_s \ll c_s^{(3)}$, while at $c_s \gg c_s^{(3)}$ it continues to increase only logarithmically. It is worth noting that at high salt concentration, $c_s \ge c_s^{(3)}$, the scaling equation for the aggregation number typical for the neutral polymeric micelles, eq 6, is recovered.

To find the dependence of the radius of the corona of an equilibrium micelle on salt concentration, we combine eqs 26 and 19 to obtain

$$R_{corona,\,eq}(c_s) \cong \begin{cases} N_A\alpha^{1/2}, & c_s \ll c_s^{(1)} \\ (N_A{}^3\alpha)^{2/11}(N_B\tau_B^2)^{2/11} c_s^{-1/11}, & c_s^{(1)} \ll c_s \ll c_s^{(2)} \\ N_A{}^{3/5}\alpha^{6/25} l_B^{-1/25}(N_B\tau_B^2)^{4/25} c_s^{-2/25} & c_s^{(2)} \ll c_s \ll c_s^{(3)} \\ N_A{}^{3/5}\alpha^{2/5}(N_B\tau_B^2)^{4/25} c_s^{-1/5}, & c_s \gg c_s^{(3)} \end{cases} \quad (27)$$

We find that an increase in the salt concentration in the range $c_s^{(1)} \ll c_s \ll c_s^{(3)}$ results in a very weak decrease in the radius of the micellar corona due to competition of (i) enhancing screening of electrostatic repulsion in the corona and (ii) increasing aggregation number. The aggregation number and the corona radius are depicted schematically in Figure 4 as a function of salt concentration.

Finally, by substituting eq 26 into eqs 20 and 23, we find the coronal contribution to the free energy of the equilibrium micelle, and using eq 2, we find the dependence of CAC on the salt concentration

$$\ln(\mathrm{CAC}) \cong -(N_B\tau_B^2)^{2/3} + \begin{cases} (N_B\tau_B^2)^{4/11}(\alpha^4 N_A)^{1/11} c_s^{-2/11}, & c_s^{(1)} \ll c_s^{(2)} \\ (N_B\tau_B^2)^{2/5}\alpha^{4/15} l_B^{-1/15} c_s^{-1/5}, & c_s^{(2)} \ll c_s \ll c_s^{(3)} \\ (N_B\tau_B^2)^{2/5}\ln(R_{corona}(c_s)/R_{core})^{2/5}, & c_s \gg c_s^{(3)} \end{cases} \quad (28)$$

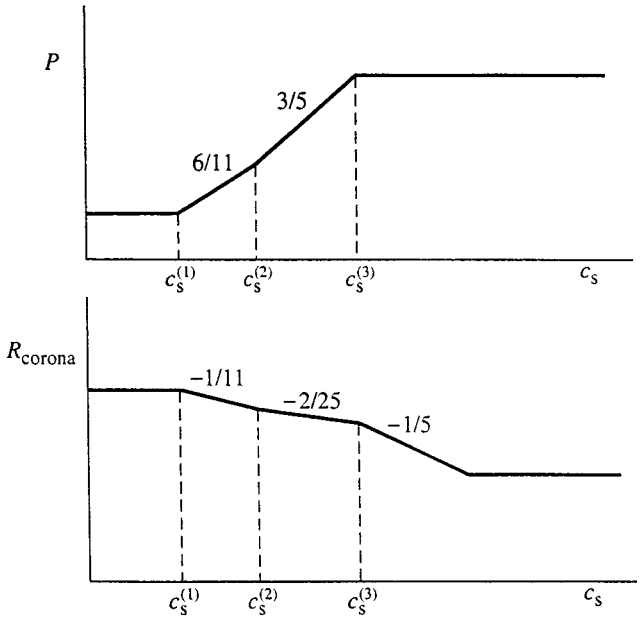

Figure 4. Schematic presentation of the dependences of an equilibrium aggregation number (a) and the radius of the micellar corona (b) for starlike micelles on salt concentration.

We therefore find that ln(CAC) decreases as a power-law function of the salt concentration in the range $c_s^{(1)} \ll c_s \ll c_s^{(3)}$ and continues to decrease, but logarithmically at $c_s^{(3)} \le c_s \le p^{-1/4}\alpha^2 N_A{}^{1/2}$.

5. Crew-Cut Polyelectrolyte Micelles

The corona of a crew-cut polyelectrolyte micelle can be viewed as a quasi-planar polyelectrolyte brush, as long as $R_{core} \gg H_{corona} \equiv R_{corona} - R_{core}$; i.e., the effect of curvature of the core interface is negligible. The structure of a planar polyelectrolyte brushes has been described in details elsewhere.[1−3] Here we present only the scaling-type arguments (cf. ref 2c) which enable us to calculate the free energy of the micellar corona with the accuracy of the leading terms and the omitted numerical prefactors.

As demonstrated in refs 1−3, there are three important length scales in the system. They are (i) the Debye screening length $r_D \cong (l_B c_s)^{-1/2}$, (ii) the surface screening length (the Gouy−Chapman length) $\lambda \cong s/l_B\alpha N_A$, and (iii) $H_0 \cong \alpha^{1/2} N_A$ which scales as the brush thickness in a salt-free solution provided that $H_0 \gg \lambda$ (the osmotic brush limit).

5.1. Micellization in a Salt-Free Solution. The equilibrium extension of the brush-forming chains in a salt-free solution is balanced by the osmotic pressure of counterions localized within the length $\sim \max\{H_0,\lambda\}$. The dominant term in the free energy per chain in the corona of the crew-cut polyelectrolyte micelle scales proportionally to the translational entropy of counterions, i.e.

$$F_{corona}/k_BT \cong \alpha N_A \begin{cases} \ln(\alpha N_A/\lambda s), & H_0 \ll \lambda \\ \ln(\alpha N_A/H_0 s), & H_0 \gg \lambda \end{cases} \quad (29)$$

When $H_0 \gg \lambda$ and the counterions are localized inside the corona of the micelle, we find $s_{eq} \cong \alpha N_A \tau_B^{-2}$ and $H_{corona} \cong N_A\alpha^{1/2}$. The aggregation number in such a

micelle can be obtained by using the packing condition 5 to give

$$p_{eq}(c_s=0) \cong \frac{(N_B\tau_B^2)^2}{(\alpha N_A)^3} \quad (30)$$

According to eq 30, the aggregation number in a crew-cut micelle strongly decreases with increasing length N_A of the coronal block.

The condition $H_{corona} \ll R_{core}$ holds as long as $N_B \gg N_A^2\alpha^{3/2}\tau_B^{-1}$, while at $N_B \ll N_A^2\alpha^{3/2}\tau_B^{-1}$ the micelles acquire a starlike shape. In the opposite limit of long B-blocks, namely at $N_B \gg N_A^3\alpha^3\tau_B^{-2}$ the entropic penalty for stretching of the insoluble blocks in the core dominates over the coronal repulsion and the universal dependence $p_{eq} \cong \tau_B^2 N_B$ is recovered.

5.2. Micellization in a Salt-Added Solution. The screening effect of added salt is important, when $r_D \le \sqrt{\lambda H_0}$ if $H_0 \gg \lambda$ or at $r_D \le H_0^2/\lambda$ if $H_0 \ll \lambda$. The brush thickness $H(c_s)$ decreases with increasing salt concentration as

$$H(c_s) \cong H_0(r_D/\sqrt{\lambda H_0})^{2/3} \cong N_A\alpha^{2/3}s^{-1/3}c_s^{-1/3} \quad (31)$$

The electrostatic interactions in the brush get screened off, and the quasi-neutral behavior (dominated by steric repulsions between the chains) is recovered at $c_s \ge \alpha^2 s^{1/2}$.

In the salt-dominated regime the interaction free energy per coronal polyelectrolyte chain decreases upon an increase in the salt concentration as

$$F_{corona}(c_s)/k_BT \cong H^2(c_s)/N_A \cong N_A(\alpha^2 c_s^{-1})^{2/3}s^{-2/3} \quad (32)$$

Assuming again the dominance of the coronal contribution to the free energy of the micelle over the free energy of the extension of the B-blocks in the core, we obtain an equilibrium area per chain

$$s_{eq}(c_s) \cong \alpha^{4/5}N_A^{3/5}\tau_B^{-6/5}c_s^{-2/5} \quad (33)$$

and an equilibrium aggregation number in a micelle

$$p_{eq}(c_s) \cong \frac{N_B^2\tau_B^{8/5}c_s^{6/5}}{\alpha^{12/5}N_A^{9/5}} \quad (34)$$

which, as expected, increases as a function of the salt concentration c_s. The corresponding exponent $^6/_5$ is remarkably larger than that in the case of a starlike micelle. This reflects stronger interactions in the quasi-planar corona of a crew-cut micelle. Again, similar to the spherical corona of a starlike micelle, the extension of the corona of a crew-cult micelle decreases with increasing c_s despite decreasing area per polyelectrolyte chain. Combining eqs 34, 5, and 31, we get

$$H_{eq}(c_s) \cong N_A^{4/5}\alpha^{2/5}\tau_B^{-6/5}c_s^{-1/5} \quad (35)$$

while the size of the core (which dominates the overall size of the crew-cut micelle) grows with increasing salt concentration $\sim p_{eq}^{1/3}(c_s) \sim c_s^{2/5}$.

At sufficiently high salt concentration the growth of the micelles is limited either by screening off of the electrostatic interactions in the corona (transition to the quasi-neutral behavior for the coronal blocks) or by the limiting extensibility of the core block; in the latter case the morphological transition from spherical to cylindrical micelles is expected to occur.

As follows from eq 33, the coronal free energy per one chain in the equilibrium crew-cut micelle scales as $\sim\tau_B^2 s_{eq} \cong \alpha^{4/5}\tau_B^{4/5}N_A^{3/5}c_s^{-2/5}$. Hence, for the CAC we find

$$\ln \mathrm{CAC} = -(N_B\tau_B^2)^{2/3} + \alpha^{4/5}\tau_B^{4/5}N_A^{3/5}c_s^{-2/5}$$

As expected, the CAC is an increasing function of the degree of ionization α and of the length of the coronal block N_A and a decreasing function of the salt concentration c_s and of the length of the core block N_B.

6. Discussion and Conclusions

We have presented the scaling theory describing the equilibrium structure of micelles formed by diblock copolymers with one hydrophobic and one polyelectrolyte block in salt-added aqueous solutions. The theory enables us to obtain the power law dependences for the main characteristics of the micelle (the aggregation number, the corona, and the core sizes) and for the CAC as a function of the length of both blocks, the degree of ionization of the polyelectrolyte block, and the concentration of added electrolyte.

As we have demonstrated above, addition of salt to the micellar solution leads to (i) decreasing CAC, (ii) increasing aggregation number in the equilibrium micelles, and (iii) weak decrease in the span of the micellar corona.

The first two trends are easily explainable, because addition of salt leads to enhancing screening of the Coulomb interactions. As the Coulomb repulsion between the coronal chains is reduced due to addition of salt, the larger number of chains can be involved in the formation of an optimal micelle (increasing aggregation number) and the lower is the free energy per chain in such a micelle (lowering of the CAC). Therefore, even when the block copolymers with a polyelectrolyte block do not form micelles in a salt-free solution, the micellization can be promoted by adding salt.

A weak decrease in the span of the micellar corona upon an increase in the salt concentration results from partial compensation of two opposing trends: addition of salt results in weakening of the Coulomb repulsion between charged monomers and, as a result, in weaker extension of the coronal chains. This effect is, however, amplified by an increase in the aggregation number (the latter results in stronger crowding of the coronal chains). Altogether, the span of the corona decreases with increasing salt concentration, but much weaker in comparison to its decrease in the micelle with fixed (quenched) number of chains.

As is illustrated in Figure 4, the effect of salt is expected to be negligible at $c_s \le c_s^{(1)}$, where $c_s^{(1)}$ is proportional to the concentration of counterions trapped inside the micellar corona. At $c_s \ge c_s^{(3)}$ screened Coulomb repulsion in the micellar corona becomes equivalent to the short-range binary repulsive interaction between monomers in a good solvent. The magnitude of the effective excluded-volume parameter is, however, determined by the degree of ionization and the salt concentration. Therefore, at $c_s \ge c_s^{(3)}$ the aggregation number acquires the same power-law dependences as in neutral block copolymer micelles, i.e., depends only logarithmically on the corona dimension and, consequently, on the salt concentration. At the same time, the span of the corona itself continues to decrease as a

power function of the salt concentration until the screened Coulomb repulsion in the corona gets weak in comparison to the steric repulsion.

The equilibrium aggregation number in polyelectrolyte micelles can be measured in experiments with quenching fluorescence, small-angle neutron (SANS), or static light (SLS) scattering. The hydrodynamic radius of the micellar corona can be independently measured in dynamic light scattering (DLS) experiments.

It is necessary to mention, however, that micelles formed in experimental systems are not always the equilibrium ones; i.e., there is no equilibrium exchange of chains between the micelles and the bulk solution. As a result, the aggregation number in these micelles does not adjust variable external conditions (e.g., temperature, salt concentration) but is predetermined by the history of the sample preparation. Sometimes in order to get micelles that are stable in a wide range of variation of the external conditions, the core-forming block with a sufficiently high T_g, such as polystyrene, is used. Polyelectrolyte micelles with a glassy cores may exhibit stability at almost constant aggregation numbers in a wide range of temperature and ionic strength variation. These micelles are reminiscent of the polyelectrolyte stars. For example, as a response to increasing ionic strength of the solution, these micelles experience much stronger contraction $R_{corona} \sim c_s^{-1/5}$ (see eq 19) as compared to the equilibrium micelles, where $R_{corona} \sim c_s^{-1/11}$, eq 27. The exponent close (although a bit weaker than) $-1/5$ for R_{corona} vs c_s has been obtained by Guenoun et al.[11e] by measuring both the hydrodynamic radius (DLS) and the gyration radius (SLS) of the NaPSS/PtBS micelles. Although the T_g for insoluble PtBS is significantly lower than the room temperature, there was no evidence of rearrangement of micelles (variation of the aggregation number) in a wide range of salt concentration, thus suggesting that these micelles were out of equilibrium.

In recent DLS experiments by Förster et al.,[28] micelles formed by block copolymers comprising poly(styrenesulfonic acid) (PSSH) as a polyelectrolyte block and poly(ethylethylene) (PEE) as a hydrophobic block have been investigated in a wide range of salt concentration. The exponent -0.13 for the hydrodynamic radius of the starlike polyelectrolyte micelle as a function of salt concentration have been found. This result is in a good agreement with our prediction, eq 27, and indicates an equilibrium nature of the (PEE−PSSH) micelles, which is most probably related to an appropriate choice of the hydrophobic block. Still more systematic experimental studies on the equilibrium polyelectrolyte micelles are necessary.

Another type of equilibrium that is not taken into account in the presented above theory is an equilibrium with respect to ionization/recombination of charged monomers with the counterions. This effect is negligible as long as the ionization constant is sufficiently high, and all the ionizable monomers in the polyelectrolyte blocks are actually ionized. The situation become more complicated for weak (so-called annealing) polyelectrolytes, like poly(acrylic acid), PAA. In the latter case the ionization constant is sufficiently small so that the degree of ionization (equal to the fraction of charged monomers in the polyelectrolyte block) depends strongly on the local concentration of hydrogen ions. The concentration of the hydrogen ions in the micellar corona is expected to be much higher than in the bulk of the solution. As a result, at pH $\sim$ pK the ionization of polyelectrolyte blocks appears to be strongly coupled to association. We shall consider these effect in our forthcoming publication.

Acknowledgment. We are thankful to T. M. Birshtein for helpful discussion and many insightful remarks. E.B.Z. acknowledges the financial support from the National Science Foundation (Grant DMR-9973300) and from the STC Program of the National Science Foundation under Agreement CHE-9876674. This work has been partially supported by the Dutch National Science Foundation (NWO) program "Self-Organization and Structure of Bionanocomposites" (No. 047.009.016).

References and Notes

(1) Pincus, P. A. *Macromolecules* **1991**, *24*, 2912. Ross, R.; Pincus, P. A. *Macromolecules* **1992**, *25*, 1503.
(2) (a) Borisov, O. V.; Birshtein, T. M.; Zhulina, E. B. *J. Phys. II* **1991**, *1*, 521. (b) Zhulina, E. B.; Borisov, O. V.; Birshtein T. M. *J. Phys. II* **1992**, *2*, 63. (c) Borisov, O. V.; Zhulina, E. B.; Birshtein T. M. *Macromolecules* **1994**, *27*, 4795.
(3) (a) Zhulina, E. B.; Borisov, O. V. *J. Chem. Phys.* **1997**, *107*, 5952. (b) Zhulina, E. B.; Klein Wolterink, J.; Borisov, O. V. *Macromolecules* **2000**, *33*, 4945.
(4) Zhulina, E. B.; Borisov, O. V. *Macromolecules* **1996**, *29*, 2618.
(5) Watanabe, H.; Patel, S. S.; Argillier, J. F.; Parsonage, E. E.; Mays, J.; Dan-Brandon, N.; Tirrell, M. *Mater. Res. Soc. Symp. Proc.* **1992**, *249*, 255.
(6) Mir, Y.; Auroy, P.; Auvray, L. *Phys. Rev. Lett.* **1995**, *75*, 2863.
(7) Guenoun, P.; Schlachli, A.; Sentenac, D.; Mays, J. W.; Benattar, J. J. *Phys. Rev. Lett.* **1995**, *74*, 3628.
(8) Ahrens, H.; Förster, S.; Helm, C. A. *Phys. Rev. Lett.* **1999**, 4798.
(9) Napperm D. H. *Polymeric Stabilization of Colloidal Dispersions*; Academic Press: London, 1985.
(10) *Stealth Liposomes*; Lasic, D., Martin, F., Eds.; CRC Press: Boca Raton, FL, 1995.
(11) (a) Kiserow, D.; Prochazka, K.; Ramireddy, C.; Tuzar, Z.; Munk, P.; Webber, S. E. *Macromolecules* **1992**, *25*, 461. (b) Khougaz, K.; Astafieva, I.; Eisenberg, A. *Macromolecules* **1995**, *28*, 7135. (c) Amiel, C.; Sikka, M.; Schneider, J. W.; Tsao, Y. H.; Tirrell, M.; Mays, J. W. *Macromolecules* **1995**, *28*, 3125. (d) Guenoun, P.; Delsanti, M.; Gaseau, D.; Auvray, L.; Cook, D. C.; Mays, J. W.; Tirrell, M *Eur. Phys. J. B* **1998**, *1*, 77. (e) Guenoun, P.; Davis, H. T.; Tirrell, M.; Mays, J. W. *Macromolecules* **1996**, *29*, 3965. (f) Guenoun, P.; Muller, F.; Delsanti, M.; Auvray, L.; Chen, Y. J. Mays, J. W.; Tirrell, M. *Phys. Rev. Lett.* **1998**, *81*, 3872. (g) Förster, S.; Hemsdorf, N.; Leube, W.; Schnablegger, H.; Regenbrecht, M.; Akari, S.; Lindner, P.; Böttcher, C. *J. Phys. Chem.* **1999**, *103*, 6657. (h) Muller, F.; Delsanti, M.; Auvray, L.; Yang, J.; Chen, Y. J.; Mays, J. W.; Demé, B.; Tirrell, M.; Guenoun, P. *Eur. Phys. J. E* **2000**, *3*, 45. (i) Groenewegen, W.; Egelhaalf, S. U.; Lapp, A.; van der Maarel, J. R. C. *Macromolecules* **2000**, *33*, 3283. Groenewegen, W.; Lapp, A.; Egelhaalf, S. U.; van der Maarel, J. R. C. *Macromolecules* **2000**, *33*, 4080.
(12) Borisov, O. V. *J. Phys. II* **1996**, *6*, 1.
(13) Borisov, O. V.; Zhulina, E. B. *Eur. Phys. J. B* **1998**, *4*, 205.
(14) Marko, J. F.; Rabin, Y. *Macromolecules* **1992**, *25*, 1503.
(15) Wittmer, J.; Joanny, J.-F. *Macromolecules* **1993**, *26*, 2691.
(16) (a) Shusharina, N. P.; Nyrkova, I. A.; Khokhlov, A. R. *Macromolecules* **1996**, *29*, 3167. (b) Shusharina, N. P.; Linse, P.; Khokhlov, A. R. *Macromolecules*, in press.
(17) Huang, C.; Olivera de la Cruz, M.; Delsanti, M.; Guenoun, P. *Macromolecules* **1997**, *30*, 8019.
(18) Dan, N.; Tirrell, M. *Macromolecules* **1993**, *26*, 4310.
(19) (a) Halperin, A. *Europhys. Lett.* **1989**, *8*, 351. (b) Halperin, A.; Alexander, S. *Macromolecules* **1989**, *22*, 2403.
(20) Birshtein, T. M.; Zhulina, E. B. *Polymer* **1989**, *30*, 170.
(21) Daoud, M.; Cotton, J. P. *J. Phys. (Paris)* **1982**, *43*, 531.
(22) Zhulina, E. B. *Polym. Sci. USSR* **1984**, *26*, 794. Birshtein, T. M.; Zhulina, E. B. *Polymer* **1984**, *25*, 1453. Birshtein, T. M.; Zhulina, E. B.; Borisov, O. V. *Polymer* **1986**, *27*, 1078.
(23) Alexander, S. *J. Phys. (Paris)* **1977**, *38*, 983.
(24) De Gennes, P.-G. *Macromolecules* **1980**, *13*, 1069.

(25) Alexander, S.; Chaikin, P. M.; Grant, P.; Morales, G. J.; Pincus, P.; Hone, D. *J. Chem. Phys.* **1984**, *80*, 5776.
(26) We remark that the uncompensated charge of the osmotic, $\mathcal{K} \gg 1$, micelle is of order $R_{\text{corona, eq}}/l_{\text{B}}$. Then the number of trapped counterions per chain is $\sim\alpha N_{\text{A}}(1 - \alpha^{-1/2} l_{\text{B}}^{-1}/p_{\text{eq}})$, and the latter term is negligible at $p_{\text{eq}} \gg \alpha^{-1/2} l_{\text{B}}^{-1}$.
(27) Murray, R. C.; Hartely, G. S. *Trans. Faraday Soc.* **1935**, *31*, 183. Konop, A. J.; Colby, R. H. *Langmuir* **1999**, *15*, 58.
(28) Förster, S.; Hermsdorf, N.; Böttcher, C.; Lindner, P. *Macromolecules*, in press.

MA010934N